FULL PAPER

Planar Tetracoordinate Carbon Atoms in M_4C Square Sheets (M = Ni, Pd, and Pt) Sandwiched between the Large π-Coordinating Ligands $[C_8H_8]^{2-}$ and $[C_9H_9]^-$

Jin-Chang Guo[a,b] and Si-Dian Li*[a,b]

Using the strategy of transition metal coordination together with that of large π-coordinating ligand complexation for planar tetracoordinate carbon (ptC) atoms, we present in this work a systematical DFT investigation on the possibility of ptC centers in M_4C square sheets sandwiched in $[C_nH_n]M_4C[C_{n'}H_{n'}]$ complexes (M = Ni, Pd, Pt; n, n' = 8, 9) with the planar π-coordinating ligands $[C_8H_8]^{2-}$ and $[C_9H_9]^-$. Introduction of a ptC center into an M_4 square sheet to form four effective ptC–M bonds helped to stabilize the

$[C_nH_n]M_4C[C_{n'}H_{n'}]$ complexes thermodynamically, and the π-coordinating $[C_8H_8]^{2-}$ and $[C_9H_9]^-$ ligands were found to match the M_4C middle decks both geometrically and electronically. Planar tetracoordinate boron (ptB) and nitrogen (ptN) behave similarly to ptC in these sandwich structures. These model sandwich complexes invite experimental syntheses and characterizations in order to open up a new area in coordination chemistry for planar tetracoordinate carbon and other non-metal atoms.

Introduction

Considerable and continuous efforts have been made to predict and produce planar tetracoordinate carbon (ptC) and planar hypercoordinate carbon atoms during the past forty years since the pioneering work by Hoffmann and co-workers in 1970;[1,2] ptC centers were observed by X-ray crystallography in stable anti-van't Hoff/LeBel compounds,[3] as exemplified by V_2(2,6-dimethoxyphenyl)$_4$·THF,[3a] $Ca_4Ni_3C_5$,[3b,3c] and $Cp_2Zr(\mu-\eta^1,\eta^2-Me_3SiCCPh)(\mu-Cl)AlMe_2$.[3d] Various electronic, mechanical, and combined approaches have been used to achieve ptCs,[4,5] including the theoretically predicted ptC-containing pentaatomic molecules,[5] which were later confirmed in the gas phase by photoelectron spectroscopy.[6] Our group proposed the possibility of transition metal coordinated ptCs in D_{4h} M_4H_4C hydridometal compounds (M = Cu, Ni);[7] ptCs centered in the bared Cu_4C^{2+} cluster and in Cu, Ag, and Au organometallic compounds were also investigated in theory.[8] The very recent discovery of the highly stable $[C_8H_8]Pd_4[C_9H_9]^+$ complex[9] with a nearly equilateral Pd_4 square sheet sandwiched between the large π-coordinating ligands $[C_8H_8]^{2-}$ and $[C_9H_9]^-$ prompted us to insert a C atom at the center of the Pd_4 unit to form a ptC-centered $[C_8H_8]Pd_4C[C_9H_9]^+$ complex. This unusual sandwich complex with the formal total valence-electron count of 60 e

turned out to be a true minimum. Using the strategy of transition metal coordination together with that of large π-coordinating ligand complexation, we systematically investigated the possibility of forming ptC centers in group 10 transition metal squares sandwiched in $[C_8H_8]M_4C[C_9H_9]^+$ and $[C_8H_8]M_4C[C_8H_8]$ complexes (M = Ni, Pd, Pt) at density functional theory (DFT) level in this work. Introducing a ptC into an M_4 square to form four effective ptC–M bonds helped to stabilize the $[C_nH_n]M_4C[C_{n'}H_{n'}]$ sandwich structures thermodynamically, and planar $[C_8H_8]^{2-}$ and $[C_9H_9]^-$ were found to be suitable ligands to flank the M_4C middle deck. Considering that Pd_4 square sheets exist stably in the sandwich-type $[C_8H_8]Pd_4[C_9H_9]^{+[9]}$ complex and that ptC-centered Ni_4C units have been observed in $Ca_4Ni_3C_5$,[3b,3c] we expected that the ptC-containing Ni_4C, Pd_4C, and Pt_4C sandwich complexes $[C_nH_n]M_4C[C_{n'}H_{n'}]$, with the stable π-coordinating $[C_8H_8]^{2-}$ and $[C_9H_9]^-$ ligands would be viable candidates to be targeted in future experiments. This strategy has been extended to planar tetracoordinate boron (ptB) and nitrogen (ptN) in the $[C_nH_n]M_4X[C_{n'}H_{n'}]$ complex series (X = B, N) in this work.

Theoretical Methods

Structural optimizations, vibrational analyses, and natural bond orbital (NBO) analyses were performed by using the hybrid B3LYP method[10] with the standard Gaussian basis of 6-311+G(3df,p) on H, B, C, N, and Ni, and with the Stuttgart quasi-relativistic pseudo-potentials and basis sets (Stuttgart RSC 1997 ECP) augmented with 2f and 1g

[a] Institute of Molecular Sciences, Shanxi University, Taiyuan 030006, Shanxi, P. R. China
[b] Institute of Material Sciences, Xinzhou Teachers University, Xinzhou 034000, Shanxi, P. R. China
⌨ Supporting information for this article is available on the WWW under http://dx.doi.org/10.1002/ejic.201000620.

functions[11] on Pd and Pt. In order to check the π-electron ring-current effects of the C_nH_n ligands, the total isotropic nucleus-independent chemical shifts (NICS) and their out-of-plane components (NICS$_{zz}$)[12] were calculated at points 0.0–5.0 Å above the ring centers along the molecular axes perpendicular to the ligand planes. NICS$_{zz}$ components are considered to better reflect the π-electron effects than NICS values at points above the ring centers where π contributions dominate.[12d–12g] The optimized ptC-centered sandwich complexes of C_s [C$_8$H$_8$]Pd$_4$C[C$_9$H$_9$]$^+$ and D_{4h} [C$_8$H$_8$]Pd$_4$C[C$_8$H$_8$] compared with the corresponding [C$_n$H$_n$]Pd$_4$[C$_{n'}$H$_{n'}$] complex, which are all true minima without imaginary frequencies at the B3LYP level, are depicted in Figure 1. The primarily ptC-related molecular orbitals (MOs) of the high-symmetry D_{4h} [C$_8$H$_8$]Pd$_4$C[C$_8$H$_8$] complex is shown in Figure 2. The detailed valence MOs of D_{4h} [C$_8$H$_8$]Pd$_4$C[C$_8$H$_8$] are depicted in the Supporting Information. The NICS and NICS$_{zz}$ scans of the Pd$_4$C-contain-

ing C_s [C$_8$H$_8$]Pd$_4$C[C$_9$H$_9$]$^+$ and D_{4h} [C$_8$H$_8$]Pd$_4$C[C$_8$H$_8$] complexes are given in Figure 3. The calculated electronic properties of the concerned complexes, including the eigenvalues of the highest occupied MOs (HOMOs), and the energy gaps between the HOMOs and the lowest unoccupied MOs (LUMOs) are given in Table 1. The first vertical ioni-
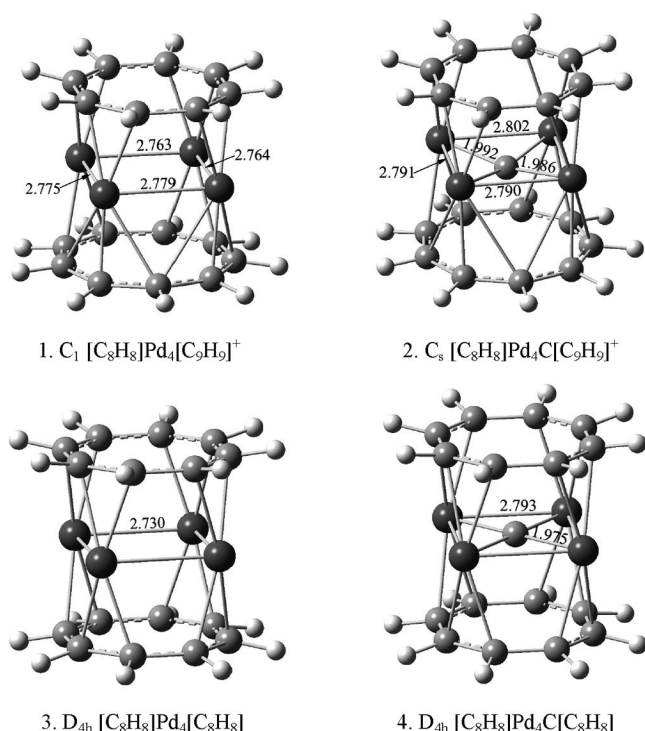
(a)

(b)

Figure 3. NICS and NICS$_{zz}$ scans of (a) C_s [C$_8$H$_8$]Pd$_4$C[C$_9$H$_9$]$^+$ (**2**) and (b) D_{4h} [C$_8$H$_8$]Pd$_4$C[C$_8$H$_8$] (**4**) compared with those of the free D_{9h} [C$_9$H$_9$]$^-$ and D_{8h} [C$_8$H$_8$]$^{2-}$ ligands, with the NICS and NICS$_{zz}$ values in ppm and the distances (d) from the ring centers in Å.

1. C_1 [C$_8$H$_8$]Pd$_4$[C$_9$H$_9$]$^+$

2. C_s [C$_8$H$_8$]Pd$_4$C[C$_9$H$_9$]$^+$

3. D_{4h} [C$_8$H$_8$]Pd$_4$[C$_8$H$_8$]

4. D_{4h} [C$_8$H$_8$]Pd$_4$C[C$_8$H$_8$]

Figure 1. Optimized geometries of the M$_4$C-centered C_s [C$_8$H$_8$]-Pd$_4$C[C$_9$H$_9$]$^+$ and D_{4h} [C$_8$H$_8$]Pd$_4$C[C$_8$H$_8$] sandwich complexes with the bond lengths around the ptC centers indicated in Å. The corresponding empty-centered [C$_n$H$_n$]Pd$_4$[C$_{n'}$H$_{n'}$] complexes are depicted for comparison.
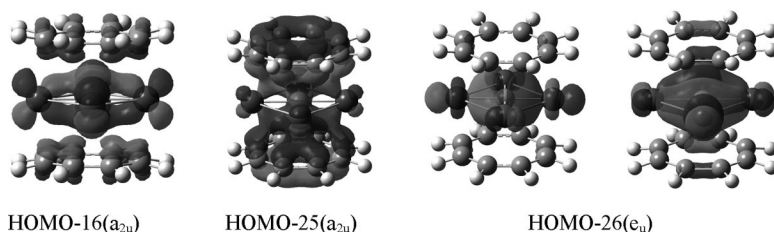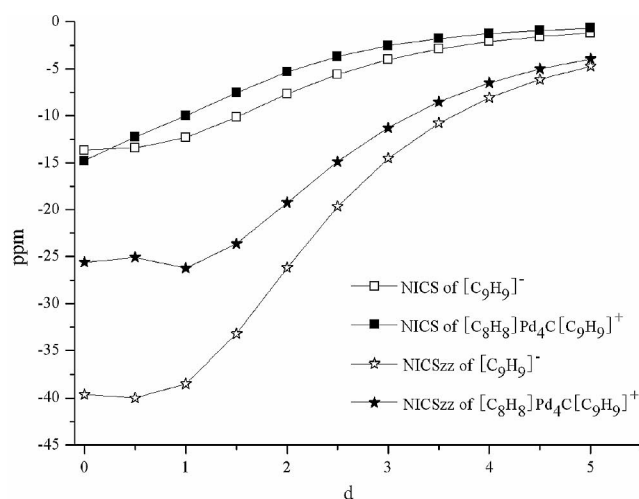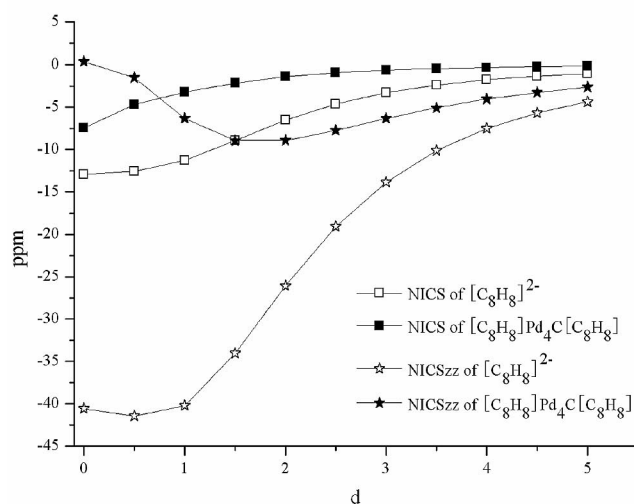
HOMO-16(a$_{2u}$) HOMO-25(a$_{2u}$) HOMO-26(e$_u$)

Figure 2. Primarily ptC-related molecular orbitals of D_{4h} [C$_8$H$_8$]Pd$_4$C[C$_8$H$_8$].

Table 1. Calculated natural atomic charges (q_{ptC}, q_M/|e|) and the total Wiberg bond indices (WBI_{ptC}, WBI_M) of the ptC centers and periphery transition metal atoms M, the Wiberg bond indices of the ptC–M interactions (WBI_{ptC-M}), NICS(1) and NICS(1)$_{zz}$ values in ppm, HOMO energies (E_{HOMO}/eV), and HOMO–LUMO energy gaps (ΔE_{gap}/eV) of the $[C_nH_n]M_4C[C_{n'}H_{n'}]$ complexes at B3LYP level. The IP values of the neutrals are also indicated in eV.

	q_{ptC}	WBI_{ptC}	q_M	WBI_M	WBI_{ptC-M}	NICS(1)	NICS(1)$_{zz}$	E_{HOMO}	ΔE_{gap}	IP
C_1 [C$_8$H$_8$]Pd$_4$[C$_9$H$_9$]$^+$			+0.42 to +0.43	1.612 to 1.614		–4.63	–4.49	–9.26	2.61	
C_s [C$_8$H$_8$]Pd$_4$C[C$_9$H$_9$]$^+$	–0.33	3.20	+0.50 to +0.51	1.70 to 1.72	0.59 to 0.60	–9.96	–26.23	–8.16	1.89	
C_s [C$_8$H$_8$]Ni$_4$C[C$_9$H$_9$]$^+$	–0.48	3.19	+0.61 to +0.62	1.88 to 1.90	0.59 to 0.62	–9.13	–19.07	–8.25	2.15	
C_s [C$_8$H$_8$]Pt$_4$C[C$_9$H$_9$]$^+$	–0.56	3.24	+0.52 to +0.53	2.14 to 2.16	0.58 to 0.62	–8.02	–21.47	–8.16	2.30	
D_{4h} [C$_8$H$_8$]Pd$_4$[C$_8$H$_8$]			+0.38	1.57		+1.52	+10.31	–5.29	2.55	6.71
D_{4h} [C$_8$H$_8$]Pd$_4$C[C$_8$H$_8$]	–0.32	3.15	+0.46	1.73	0.59	–3.21	–6.32	–4.35	1.92	5.71
D_{4h} [C$_8$H$_8$]Ni$_4$C[C$_8$H$_8$]	–0.47	3.14	+0.57	1.88	0.59	–5.15	–7.01	–4.18	2.27	5.30
C_{4v} [C$_8$H$_8$]Pt$_4$C[C$_8$H$_8$]	–0.57	3.21	+0.47	2.15	0.60	–4.88	–12.75	–4.33	2.05	5.76

zation potentials (IPs) of the neutrals were calculated as the energy differences between the neutrals and the corresponding cations in the optimized neutral structures. We mainly focused on the ptC-containing M$_4$C complexes (M = Pd, Ni, Pt) in the following discussions, and especially on the experimentally closely related Pd$_4$C series. Results on ptB-centered M$_4$B and ptN-centered M$_4$N complexes are also summarized in the Supporting Information. All the calculations in this work were carried out by using the Gaussian 03 program.[13]

Results and Discussion

Similarl to the experimentally known C_1 [C$_8$H$_8$]Pd$_4$-[C$_9$H$_9$]$^+$ (1),[9] the ptC-centered C_s [C$_8$H$_8$]Pd$_4$C[C$_9$H$_9$]$^+$ (2) possesses a typical sandwich structure with the C$_8$H$_8$ ring coordinating to the nearly equilateral Pd$_4$C square sheet in a μ_4-η^2:η^2:η^2:η^2 mode ($r_{Pd-C(C8H8)}$ = 2.32–2.34 Å) and C$_9$H$_9$ in a μ_4-η^2:η^2:η^3:η^3 mode ($r_{Pd-C(C9H9)}$ = 2.40 and 2.47 Å for η^2-Pd; $r_{Pd-C(C9H9)}$ = 2.62, 2.39, and 2.85 Å for η^3-Pd, with one C atom on the C$_9$H$_9$ ring coordinating to two Pd atoms with the longest Pd–C distances). The ptC-centered C_s 2 has an average Pd–Pd distance of 2.79 Å, which is 0.07 Å longer than the measured value of 2.72 Å in C_1 [C$_8$H$_8$]Pd$_4$[C$_9$H$_9$]$^+$.[9] The calculated ptC–Pd distances of r_{ptC-Pd} = 1.986 and 1.992 Å in C_s 2 were shorter than the sum of the covalent radii of Pd and C (2.14 Å), indicating that effective ptC–Pd bonds have been formed around the ptC center. The calculated total atomic Wiberg bond order of WBI_{ptC} = 3.20 and the individual bond orders of WBI_{ptC-Pd} = 0.59–0.60 generally agree with the ptC-related bond orders reported in the literature.[1–8] These values also indicate that multicenter interactions, which are not included in the calculation of individual WBI_{ptC-Pd}, make considerable contribution to the chemical bonding in this complex. The low natural atomic charges of q_{ptC} = –0.33 |e| and q_{Pd} = +0.50 to +0.51 |e| suggest that the ptC–Pd interactions are mainly covalent in C_s 2. The periphery Pd atoms have the calculated total bond order of WBI_{Pd} = 1.70–1.72. Triplet and quintet sandwich isomers were found to be considerably less stable than singlet C_s 2 at the same theoretical level. Similar results have been obtained for C_s [C$_8$H$_8$]-Ni$_4$C[C$_9$H$_9$]$^+$ with r_{ptC-Ni} = 1.813 and 1.820 Å and C_s [C$_8$H$_8$]Pt$_4$C[C$_9$H$_9$]$^+$ with r_{ptC-Pt} = 2.053 and 2.067 Å.

Flanking a Pd$_4$ square with two equivalent C$_8$H$_8$ rings in a μ_4-η^2:η^2:η^2:η^2 mode produces the sandwich-like D_{4h} [C$_8$H$_8$]Pd$_4$[C$_8$H$_8$] (3) that has a Pd–Pd bond length of r_{Pd-Pd} = 2.730 Å. Inserting a ptC at the center of D_{4h} 3, the highly symmetrical D_{4h} [C$_8$H$_8$]Pd$_4$C[C$_8$H$_8$] (4), which contains a perfect Pd$_4$C square, is obtained. The ptC-centered D_{4h} 4 has 60 valence electrons and possesses bond lengths of r_{Pd-Pd} = 2.793 Å and r_{ptC-Pd} = 1.975 Å and bond orders of WBI_{Pd} = 1.73, WBI_{ptC} = 3.15, and WBI_{ptC-Pd} = 0.59. Typical coordination bonds are formed between the Pd$_4$C core and the two [C$_8$H$_8$]$^{2-}$ ligands ($r_{Pd-C(C8H8)}$ = 2.392 Å and $WBI_{Pd-C(C8H8)}$ = 0.16). Interestingly, the two C$_8$H$_8$ rings in D_{4h} 4 exhibit certain bond length alternations ($r_{C=C}$ = 1.402 Å and r_{C-C} = 1.458 Å) with an averaged C–C distance of r_{C-C} = 1.430 Å, which is 0.016 Å longer than the corresponding value of r_{C-C} = 1.414 Å in a perfect D_{8h} [C$_8$H$_8$]$^{2-}$ dianion[14] at the same B3LYP level. The C–C bond-length alternation in $[C_nH_n]M_4C[C_{n'}H_{n'}]$ complexes studied in this work is related to the fact that each periphery transition metal atom in these M$_4$C square sheets is coordinated in a η^2 mode to two C=C pπ–pπ bonds above and below it (see Figure 1). The perfect D_{4h} [C$_8$H$_8$]Ni$_4$C[C$_8$H$_8$] complex and the slightly distorted C_{4v} [C$_8$H$_8$]Pt$_4$C[C$_8$H$_8$] complex behave similarly to D_{4h} 4. A perfect D_{4h} [C$_8$H$_8$]-Pt$_4$C[C$_8$H$_8$] complex proved to be a transition state leading to the C_{4v} geometry that contains a quasi-ptC center lying 0.271 Å above the Pt$_4$ plane (see detailed coordinates in Supporting Information).

With one less and one more valence electron than C both B and N, respectively, can be used to substitute the ptC centers in C_s 2 and D_{4h} 4 to produce the isoelectronic ptB-containing C_s [C$_8$H$_8$]Pd$_4$B[C$_9$H$_9$] complex, the slightly distorted ptN-containing C_1 [C$_8$H$_8$]Pd$_4$N[C$_9$H$_9$]$^{2+}$ complex, the ptB-containing D_{2d} [C$_8$H$_8$]Pd$_4$B[C$_8$H$_8$]$^-$ complex, and the ptN-containing D_{2d} [C$_8$H$_8$]Pd$_4$N[C$_8$H$_8$]$^+$ complex (see details in Supporting Information). These ptB- and ptN-containing sandwich complexes all were found to be true minima similar to the corresponding ptC-containing complexes. For example, the bond lengths and the bond orders in the high-symmetry [C$_8$H$_8$]Pd$_4$X[C$_8$H$_8$] complexes (X = B, C, N) (r_{Pd-Pd} = 2.819 Å, r_{ptB-Pd} = 1.993 Å, WBI_{ptB} = 3.20, and WBI_{ptB-Pd} = 0.54 for D_{2d} [C$_8$H$_8$]Pd$_4$B[C$_8$H$_8$]$^-$; r_{Pd-Pd} = 2.857 Å, r_{ptN-Pd} = 2.020 Å, WBI_{ptN} = 2.47, and WBI_{ptN-Pd} = 0.41 for D_{2d} [C$_8$H$_8$]Pd$_4$N[C$_8$H$_8$]$^+$) compare

favourably with those obtained for D_{4h} [C_8H_8]Pd$_4$C[C_8H_8] (**4**) (r_{Pd-Pd} = 2.793 Å, r_{ptC-Pd} = 1.975 Å, WBI$_{ptC}$ = 3.15, and WBI$_{ptC-Pd}$ = 0.59). The low covalent bond order of the ptN center can be explained by the relatively strong ionic interaction formed between the highly negatively charged ptN center (q_{ptN} = –0.97 |e|) and the four positively charged Pd periphery atoms (q_{Pd} = +0.65 |e|). Similar situations exist for the low-symmetry [C_8H_8]Pd$_4$X[C_9H_9] series (X = B, C, N).

Orbital analyses can be used to explain the bonding nature of these ptC centers. The atomic electron configurations of the ptC [He]$2s^{1.83}2p^{2.42}(2s^{1.83}2p_x^{0.69}2p_y^{0.81}2p_z^{0.91})$ in C_s **2** and the ptC [He]$2s^{1.87}2p^{2.36}(2s^{1.87}2p_x^{0.93}p_y^{0.93}p_z^{0.51})$ in D_{4h} **4** reveal significant ptC $2p_z$ occupation in agreement with the Wang–Schleyer ptC bonding model, which is based conceptually on stabilization of the vacant ptC $2p_z$ through electron transfer.[8a,15] PtC serves as a σ-acceptor and a π-donor in planar tetra- and hypercoordinate carbon systems.[1–8,16] As shown in Figure 2, both the HOMO-16(a_{2u}) and HOMO-25(a_{2u}) of D_{4h} [C_8H_8]Pd$_4$C[C_8H_8] (**4**) contain an in-phase π-overlap between the ptC $2p_z$ and the four equivalent periphery Pd 4d orbitals, while the delocalized π MOs of the [C_8H_8]$^{2-}$ ligands form an antibonding interaction with the Pd$_4$C middle deck in the former and a bonding interaction in the latter. The all-in-phase bonding HOMO-25(a_{2u}) involves a weak overlap between the ptC $2p_z$ orbital and the delocalized π MOs of the ligands, which is expected to promote the ring-current effects of the C_8H_8 rings. The degenerate HOMO-26(e_u) represents two effective σ-bonds between the ptC $2p_x2p_y$ and the Pd 4d orbitals in radial directions in the Pd$_4$C plane, with the corresponding antibonding orbitals LUMO+2(e_u) unoccupied (see Supporting Information). The in-phase bonding MOs of HOMO-13(b_{1g}), the degenerate HOMO-22(e_u), and HOMO-27(a_{1g}) mainly represent the Pd(d_{z^2})–ligand(π) coordination interactions in the vertical direction (see Supporting Information). Similar electronic configurations and ptC-related MOs exist in C_s **2** and other ptC-centered sandwich complexes.

As shown in Figure 3, the NICS values of the free 10π [C_9H_9]$^-$ (D_{9h}) and [C_8H_8]$^{2-}$ (D_{8h}) rings increase monotonically, while their NICS$_{zz}$ components exhibit only very shallow minima at points 0.5–1.0 Å above the ring centers, unlike the prototypical free 6π C_6H_6 (D_{6h}) ring, which possesses deep minima at both NICS(1) and NICS(1)$_{zz}$.[12g] The C_9H_9 ring in the C_s **2** complex behaves quite similarly to the free D_{9h} [C_9H_9]$^-$ ligand for both NICS and NICS$_{zz}$ [see Figure 3(a)]. The conventional values of NICS(1) = –9.96 ppm and NICS(1)$_{zz}$ = –26.23 ppm compare favourably, albeit systematically lower, with NICS(1) = –12.32 ppm and NICS(1)$_{zz}$ = –38.49 ppm obtained for the free [C_9H_9]$^-$. For the C_8H_8 rings in the D_{4h} [C_8H_8]-Pd$_4$C[C_8H_8] (**4**) complex, which possesses C–C bond length alternation, the calculated NICS and NICS$_{zz}$ values are less negative than the corresponding values obtained for the free [C_8H_8]$^{2-}$ ligand between 0.0 and 2.0 Å above the ring center [see Figure 3(b) and Table 1]. NBO analyses indicated that a π-donating C_8H_8 ring in the neutral D_{4h} [C_8H_8]-

Pd$_4$C[C_8H_8] (**4**) complex carries a net natural charge of $q_{[C8H8]}$ = –1.08 |e|, a value much smaller than the formal charge ($q_{[C8H8]}$ = –2.0 |e|) of a free D_{8h} [C_8H_8]$^{2-}$, which results in significantly less effective ring-current effects and therefore less negative NICS and NICS$_{zz}$ values for the complex. The charge transfers from the M$_4$C middle sheets are not effective enough to fully satisfy the formal charge states of [C_9H_9]$^-$ and [C_8H_8]$^{2-}$ for the large carbocyclic ligands in the complexes. Nevertheless, the overall variation and convergence behavior of the ligands in the complexes and in the free gas states appear to be similar (Figure 3). The ptC-centered [C_nH_n]M$_4$C[$C_{n'}H_{n'}$] complexes have more negative NICS(1) and NICS(1)$_{zz}$ values than the corresponding empty-centered [C_nH_n]M$_4$[$C_{n'}H_{n'}$] complexes (see Table 1), indicating that the ptC centers help to promote the ring-current effects of the ligands in these complexes, which is in agreement with the orbital analyses presented above.

To check the thermodynamic stability of the ptC-containing complexes, we calculated the "insertion energies" of the ptC centers (ΔE_{ptC}) in the following processes.

$$[C_8H_8]M_4[C_9H_9]^+ + C = [C_8H_8]M_4C[C_9H_9]^+ \tag{1}$$

$$[C_8H_8]M_4[C_8H_8] + C = [C_8H_8]M_4C[C_8H_8] \tag{2}$$

We found them to be ΔE_{ptC} = –83.3, –51.7, and –56.0 kcal mol^{-1} in (1) and ΔE_{ptC} = –74.0, –41.2, and –42.8 kcal mol^{-1} in (2) for M = Ni, Pd, and Pt, respectively. These negative energy changes indicate that the insertion of a ptC atom to form four effective ptC–M bonds helps to stabilize the [C_8H_8]M$_4$C[C_9H_9]$^+$ and [C_8H_8]M$_4$C[C_8H_8] complexes thermodynamically. It is worth noting that the ptCs in the Ni$_4$C squares possess significantly higher insertion energies than in both Pd$_4$C and Pt$_4$C in these processes. An Ni$_4$ square best matches in size both the ptC center and the carbocyclic C_nH_n ligands (n = 8, 9) in the [C_nH_n]-M$_4$C[$C_{n'}H_{n'}$] series (M = Ni, Pd, and Pt). This observation supports the fact that ptC centers have already been observed in square Ni$_4$C in crystalline Ca$_4$Ni$_3$C$_5$[3b,3c] and have been predicted as possible in the hydridonickel compound Ni$_4$H$_4$C.[7] As indicated in Table 1, these ptC-centered complexes also possess considerably low HOMO energies (E_{HOMO} = –4.2 to –8.3 eV) and wide HOMO–LUMO energy gaps (ΔE_{gap} = 1.9–2.3 eV), further supporting their thermodynamic stability. The [C_8H_8]M$_4$C[C_8H_8] neutrals all have relatively high ionization potentials, with the calculated IPs = 5.30–5.76 eV at the DFT level. Vibrational analysis showed that these ptC-containing complexes possess a characteristic ptC–M in-plane stretching vibrational frequency at approximately 500 cm^{-1}, which is absent in the corresponding empty-centered systems (see Figure S1 in the Supporting Information).

Conclusions

In this work, we have performed a systematical DFT investigation on the possibility of ptC-centered [C_nH_n]-M$_4$C[$C_{n'}H_{n'}$] sandwich complexes (M = Ni, Pd, Pt; n, n' =

8, 9) with the large π-coordinating $[C_8H_8]^{2-}$ and $[C_9H_9]^{-}$ ligands. Introduction of a ptC center into a square M_4 sheet to form four effective ptC–M bonds helps to stabilize the $[C_nH_n]M_4C[C_{n'}H_{n'}]$ complexes thermodynamically, and the $[C_8H_8]^{2-}$ and $[C_9H_9]^{-}$ ligands were found to match the M_4C middle decks both geometrically and electronically; ptB and ptN centers behave similarly to ptC centers with certain structural distortions. These novel sandwich complexes invite experimental syntheses and characterizations in order to open up a new area in coordination chemistry for ptC and other planar tetracoordinate atoms.

Supporting Information (see footnote on the first page of this article): Calculated IR spectra of C_s $[C_8H_8]Pd_4C[C_9H_9]^{+}$ and C_1 $[C_8H_8]Pd_4[C_9H_9]^{+}$, valence MOs of D_{4h} $[C_8H_8]Pd_4C[C_8H_8]$, lowest vibrational frequencies, zero point energies, and optimized coordinates of the $[C_nH_n]M_4X[C_{n'}H_{n'}]$ and $[C_nH_n]M_4[C_{n'}H_{n'}]$ complexes (X = C, B, N).

[1] a) R. Hoffmann, R. W. Alder Jr., C. F. Wilcox, *J. Am. Chem. Soc.* **1970**, *92*, 4992; b) J. B. Collins, J. D. Dill, E. D. Jemmis, Y. Apeloig, P. v. R. Schleyer, R. Seeger, J. A. Pople, *J. Am. Chem. Soc.* **1976**, *98*, 5419.

[2] a) R. Keese, *Chem. Rev.* **2006**, *106*, 4787; b) V. I. Minkin, R. M. Minyaev, R. Hoffmann, *Russ. Chem. Rev.* **2002**, *71*, 869; c) L. Radom, D. Rasmussen, *Pure Appl. Chem.* **1998**, *70*, 1977; d) K. Sorger, P. v. R. Schleyer, *THEOCHEM* **1995**, *338*, 317; e) D. Röttger, G. Erker, *Angew. Chem. Int. Ed. Engl.* **1997**, *36*, 812; f) W. Siebert, A. Gunale, *Chem. Soc. Rev.* **1999**, *28*, 367; g) G. Erker, *Chem. Soc. Rev.* **1999**, *28*, 307; h) G. Merino, M. A. Mendez-Rojas, A. Vela, T. Heine, *J. Comput. Chem.* **2007**, *28*, 362; i) K. Exner, P. v. R. Schleyer, *Science* **2000**, *290*, 1937; j) Z.-X. Wang, P. v. R. Schleyer, *Science* **2001**, *292*, 2645.

[3] a) F. A. Cotton, M. J. Millar, *J. Am. Chem. Soc.* **1977**, *99*, 7886; b) U. E. Musanke, W. Jeitschko, *Z. Naturforsch., Teil B* **1991**, *46*, 1177; c) E. F. Merschrod, S. H. Tang, R. Hoffmann, *Z. Naturforsch., Teil B* **1998**, *53*, 322; d) G. Erker, R. Zwettler, C. Kruger, R. Noe, S. Werner, *J. Am. Chem. Soc.* **1990**, *112*, 9620; e) G. Erker, M. Albrecht, C. Kruger, S. Werner, *Organometallics* **1991**, *10*, 3791; f) M. Albrecht, G. Erker, C. Kruger, *SYNLETT* **1993**, *7*, 441; g) G. Erker, *Comments Inorg. Chem.* **1992**, *13*, 111; h) C. H. Suresh, G. Frenking, *Organometallics*, DOI: 10.1021/om100260p.

[4] See recent papers: a) Y. Wang, *J. Comput. Chem.* **2009**, *30*, 2122; b) C. Zhang, W. Sun, Z. Cao, *J. Am. Chem. Soc.* **2008**, *130*, 5638; c) Z.-X. Wang, C.-G. Zhang, Z. Chen, P. v. R. Schleyer, *Inorg. Chem.* **2008**, *47*, 1332; d) K. Ito, Z. Chen, C. Corminboeuf, C. S. Wannere, X. H. Zhang, Q. S. Li, P. v. R. Schleyer, *J. Am. Chem. Soc.* **2007**, *129*, 1510; e) G. Merino, M. A. Mendez-Rojas, H. I. Beltran, C. Corminboeuf, T. Heine, A. Vela, *J. Am. Chem. Soc.* **2004**, *126*, 16160; f) Z.-X. Wang, P. v. R. Schleyer, *J. Am. Chem. Soc.* **2002**, *124*, 11979.

[5] a) P. v. R. Schleyer, A. I. Boldyrev, *J. Chem. Soc., Chem. Commun.* **1991**, 1536; b) A. I. Boldyrev, J. Simons, *J. Am. Chem. Soc.* **1998**, *120*, 7967.

[6] a) X. Li, L.-S. Wang, A. I. Boldyrev, J. Simons, *J. Am. Chem. Soc.* **1999**, *121*, 6033; b) L.-S. Wang, A. I. Boldyrev, X. Li, J. Simons, *J. Am. Chem. Soc.* **2000**, *122*, 7681; c) X. Li, H. J. Zhai,

L.-S. Wang, *Chem. Phys. Lett.* **2002**, *357*, 415; d) X. Li, H.-F. Zhang, L.-S. Wang, G. D. Geske, A. I. Boldyrev, *Angew. Chem.* **2000**, *112*, 3776; *Angew. Chem. Int. Ed.* **2000**, *39*, 3630.

[7] a) S.-D. Li, G.-M. Ren, C.-Q. Miao, Z.-H. Jin, *Angew. Chem. Int. Ed.* **2004**, *43*, 1371; b) S.-D. Li, G.-M. Ren, C.-Q. Miao, *J. Phys. Chem. A* **2005**, *109*, 259; c) Y.-B. Wu, C.-X. Yuan, F. Gao, H.-G. Lu, J.-C. Guo, S.-D. Li, Y.-K. Wang, P. Yang, *Organometallics* **2007**, *26*, 4395.

[8] a) D. Roy, C. Corminboeuf, C. S. Wannere, R. B. King, P. v. R. Schleyer, *Inorg. Chem.* **2006**, *45*, 8902; b) M.-D. Su, *Inorg. Chem.* **2005**, *44*, 4829.

[9] T. Murahashi, R. Inoue, K. Usui, S. Ogoshi, *J. Am. Chem. Soc.* **2009**, *131*, 9888.

[10] a) A. D. Becke, *J. Chem. Phys.* **1993**, *98*, 5648; b) C. Lee, W. Yang, R. G. Parr, *Phys. Rev. B* **1988**, *37*, 785.

[11] a) D. Feller, *J. Comput. Chem.* **1996**, *17*, 1571; b) K. L. Schuchardt, B. T. Didier, T. Elsethagen, L. Sun, V. Gurumoorthi, J. Chase, J. Li, T. L. Windus, *J. Chem. Inf. Model.* **2007**, *47*, 1045; c) J. M. L. Martin, A. Sundermann, *J. Chem. Phys.* **2001**, *114*, 3408.

[12] a) P. v. R. Schleyer, C. Maerker, A. Dransfeld, H. Jiao, N. J. R. E. Hommes, *J. Am. Chem. Soc.* **1996**, *118*, 6317; b) P. v. R. Schleyer, H. Jiao, N. J. R. E. Hommes, V. G. Malkin, O. L. Malkina, *J. Am. Chem. Soc.* **1997**, *119*, 12669; c) P. v. R. Schleyer, M. Manoharan, Z.-X. Wang, B. Kiran, H. Jiao, R. Puchta, N. J. R. E. Hommes, *Org. Lett.* **2001**, *3*, 2465; d) H. Fallah-Bagher-Shaidaei, C. S. Wannere, C. Corminboeuf, R. Puchta, P. v. R. Schleyer, *Org. Lett.* **2006**, *8*, 863; e) Z. Chen, C. S. Wannere, C. Corminboeuf, R. Puchta, P. v. R. Schleyer, *Chem. Rev.* **2005**, *105*, 3842; f) C. Corminboeuf, T. Heine, G. Seifert, P. v. R. Schleyer, *Phys. Chem. Chem. Phys.* **2004**, *6*, 273; g) A. Stanger, *J. Org. Chem.* **2006**, *71*, 883.

[13] M. J. Frisch, G. W. Trucks, H. B. Schlegel, G. E. Scuseria, M. A. Robb, J. R. Cheeseman, J. A. Montgomery Jr., T. Vreven, K. N. Kudin, J. C. Burant, J. M. Millam, S. S. Iyengar, J. Tomasi, V. Barone, B. Mennucci, M. Cossi, G. Scalmani, N. Rega, G. A. Petersson, H. Nakatsuji, M. Hada, M. Ehara, K. Toyota, R. Fukuda, J. Hasegawa, M. Ishida, T. Nakajima, Y. Honda, O. Kitao, H. Nakai, M. Klene, X. Li, J. E. Knox, H. P. Hratchian, J. B. Cross, C. Adamo, J. Jaramillo, R. Gomperts, R. E. Stratmann, O. Yazyev, A. J. Austin, R. Cammi, C. Pomelli, J. W. Ochterski, P. Y. Ayala, K. Morokuma, G. A. Voth, P. Salvador, J. J. Dannenberg, V. G. Zakrzewski, S. Dapprich, A. D. Daniels, M. C. Strain, O. Farkas, D. K. Malick, A. D. Rabuck, K. Raghavachari, J. B. Foresman, J. V. Ortiz, Q. Cui, A. G. Baboul, S. Clifford, J. Cioslowski, B. B. Stefanov, G. Liu, A. Liashenko, P. Piskorz, I. Komaromi, R. L. Martin, D. J. Fox, T. Keith, M. A. Al-Laham, C. Y. Peng, A. Nanayakkara, M. Challacombe, P. M. W. Gill, B. Johnson, W. Chen, M. W. Wong, C. Gonzalez, J. A. Pople, *Gaussian 03, Revision A.1*, Gaussian, Inc., Pittsburgh, PA, **2003**.

[14] a) I. Bach, K.-R. Porschke, B. Proft, R. Goddard, C. Kopiske, C. Kruger, A. Rufinska, K. Seevogel, *J. Am. Chem. Soc.* **1997**, *119*, 3773; b) S. C. A. H. Pierrefixe, F. M. Bickelhaupt, *J. Phys. Chem. A* **2008**, *112*, 12816; c) M. D. Walter, G. Wolmershauser, H. Sitzmann, *J. Am. Chem. Soc.* **2005**, *127*, 17494.

[15] Z.-X. Wang, P. v. R. Schleyer, *J. Am. Chem. Soc.* **2001**, *123*, 994.

[16] Y. Pei, W. An, K. Ito, P. v. R. Schleyer, X. C. Zeng, *J. Am. Chem. Soc.* **2008**, *130*, 10394.